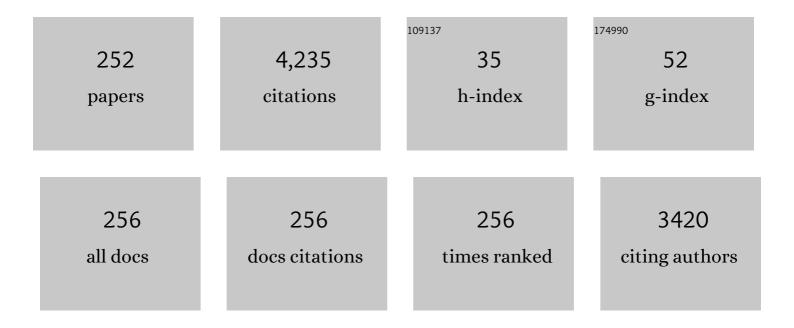
List of Publications by Year in descending order

Source: https://exaly.com/author-pdf/5249685/publications.pdf Version: 2024-02-01



#	Article	IF	CITATIONS
1	Therapeutic Targets and Emerging Treatments in Advanced Chondrosarcoma. International Journal of Molecular Sciences, 2022, 23, 1096.	1.8	17
2	Pretreatment Neutrophil Count and Platelet-lymphocyte Ratio as Predictors of Metastasis in Patients With Osteosarcoma. Anticancer Research, 2022, 42, 1081-1089.	0.5	7
3	A scoring system combining clinical, radiological, and histopathological examinations for differential diagnosis between lipoma and atypical lipomatous tumor/well-differentiated liposarcoma. Scientific Reports, 2022, 12, 237.	1.6	13
4	Primary total knee arthroplasty assisted by computed tomography-free navigation for secondary knee osteoarthritis following massive calcium phosphate cement packing for distal femoral giant-cell bone tumor treatment: a case report. BMC Musculoskeletal Disorders, 2022, 23, 170.	0.8	0
5	Synchronous chondroblastomas in the knee joint: A case report. International Journal of Surgery Case Reports, 2022, 95, 107264.	0.2	0
6	Therapeutic effects and clinical outcomes of immune checkpoint inhibitors on bone metastases in lung cancer Journal of Clinical Oncology, 2022, 40, e21118-e21118.	0.8	0
7	Clinical outcomes and life expectancy of patients with unplanned excisions of soft tissue sarcoma Journal of Clinical Oncology, 2022, 40, e23554-e23554.	0.8	1
8	Compartment-specific clinical outcomes in patients with soft tissue sarcomas of the thigh Journal of Clinical Oncology, 2022, 40, e23549-e23549.	0.8	0
9	Novel predictors associated with therapeutic effects of immune checkpoint inhibitors on bone metastasis of non-small cell lung cancer Journal of Clinical Oncology, 2022, 40, e21071-e21071.	0.8	0
10	Diagnostic accuracies of intraoperative frozen section and permanent section examinations for histological grades during open biopsy of bone tumors. International Journal of Clinical Oncology, 2021, 26, 613-619.	1.0	6
11	Multikinase-Inhibitor Screening in Drug-resistant Osteosarcoma Patient-derived Orthotopic Xenograft Mouse Models Identifies the Clinical Potential of Regorafenib. Cancer Genomics and Proteomics, 2021, 18, 637-643.	1.0	4
12	The number of osteoclasts in a biopsy specimen can predict the efficacy of neoadjuvant chemotherapy for primary osteosarcoma. Scientific Reports, 2021, 11, 1989.	1.6	6
13	Reconstruction using a frozen autograft for a skull and humeral lesion of synchronous multicentric osteosarcoma after undergoing successful neoadjuvant chemotherapy: a case report and review of the literature. BMC Surgery, 2021, 21, 56.	0.6	4
14	Long-term survival in a patient with Hutchinson-Gilford progeria syndrome and osteosarcoma: A case report. World Journal of Clinical Cases, 2021, 9, 854-863.	0.3	0
15	Abscopal Effect of Frozen Autograft Reconstruction Combined with an Immune Checkpoint Inhibitor Analyzed Using a Metastatic Bone Tumor Model. International Journal of Molecular Sciences, 2021, 22, 1973.	1.8	3
16	Combination Methionine-methylation-axis Blockade: A Novel Approach to Target the Methionine Addiction of Cancer. Cancer Genomics and Proteomics, 2021, 18, 113-120.	1.0	12
17	Associations of PD-L1, PD-L2, and HLA class I expression with responses to immunotherapy in patients with advanced sarcoma: post hoc analysis of a phase 1/2 trial. Clinical and Translational Oncology, 2021, 23, 1620-1629.	1.2	2
18	Significant Improvement After Surgery for a Symptomatic Osteoblastoma in a Patient with Camurati–Engelmann Disease: Case Report and Literature Review. Calcified Tissue International, 2021, 108, 819-824.	1.5	1

#	Article	lF	CITATIONS
19	Bone and Soft Tissue Tumors: New Treatment Approaches. Cancers, 2021, 13, 1832.	1.7	4
20	Delayed Initiation of Treatment Is Associated With Metastasis of Malignant Bone Tumor. Anticancer Research, 2021, 41, 2993-2999.	0.5	3
21	A Radiological Scoring System for Differentiation between Enchondroma and Chondrosarcoma. Cancers, 2021, 13, 3558.	1.7	6
22	Clinical outcomes of frozen autograft reconstruction for the treatment of primary bone sarcoma in adolescents and young adults. Scientific Reports, 2021, 11, 17291.	1.6	8
23	MSX2 inhibits the growth and migration of osteosarcoma cells by repressing SOX2. American Journal of Translational Research (discontinued), 2021, 13, 5851-5865.	0.0	2
24	Osteosarcoma Patient-derived Orthotopic Xenograft (PDOX) Models Used to Identify Novel and Effective Therapeutics: A Review. Anticancer Research, 2021, 41, 5865-5871.	0.5	13
25	Clinical characteristics of patients with undergoing unplanned excisions of malignant soft tissue tumors. Journal of Orthopaedic Surgery, 2021, 29, 230949902110575.	0.4	4
26	Patient-derived orthotopic xenograft models of sarcoma. Cancer Letters, 2020, 469, 332-339.	3.2	17
27	The combination of oral-recombinant methioninase and azacitidine arrests aÂchemotherapy-resistant osteosarcoma patient-derived orthotopic xenograft mouse model. Cancer Chemotherapy and Pharmacology, 2020, 85, 285-291.	1.1	27
28	The process of bone regeneration from devitalization to revitalization after pedicle freezing with immunohistochemical and histological examination in rabbits. Cryobiology, 2020, 92, 130-137.	0.3	10
29	Combination of oral recombinant methioninase and decitabine arrests a chemotherapy-resistant undifferentiated soft-tissue sarcoma patient-derived orthotopic xenograft mouse model. Biochemical and Biophysical Research Communications, 2020, 523, 135-139.	1.0	15
30	PPARÎ ³ Agonist Pioglitazone in Combination With Cisplatinum Arrests a Chemotherapy-resistant Osteosarcoma PDOX Model. Cancer Genomics and Proteomics, 2020, 17, 35-40.	1.0	24
31	Secondary Osteoarthritis After Curettage and Calcium Phosphate Cementing for Giant-Cell Tumor of Bone Around the Knee Joint. JBJS Open Access, 2020, 5, e19.00068-e19.00068.	0.8	9
32	Osimertinib regressed an EGFR-mutant lung-adenocarcinoma bone-metastasis mouse model and increased long-term survival. Translational Oncology, 2020, 13, 100826.	1.7	6
33	Atypical and incomplete pulmonary hypertrophic osteoarthropathy in the left distal femur: a case report. BMC Surgery, 2020, 20, 293.	0.6	0
34	Diagnosis and treatment of intramedullary osteosclerosis: a report of three cases and literature review. BMC Musculoskeletal Disorders, 2020, 21, 762.	0.8	3
35	Clinical course of grafted cartilage in osteoarticular frozen autografts for reconstruction after resection of malignant bone and soft-tissue tumor involving an epiphysis. Journal of Bone Oncology, 2020, 24, 100310.	1.0	10
36	Accuracy of histological grades from intraoperative frozen-section diagnoses of soft-tissue tumors. International Journal of Clinical Oncology, 2020, 25, 2158-2165.	1.0	6

#	Article	IF	CITATIONS
37	Risk Factors for Postoperative Deep Infection After Malignant Bone Tumor Surgery of the Extremities. Anticancer Research, 2020, 40, 3551-3557.	0.5	8
38	Intraoperative ultrasonographyâ€guided surgery for malignant soft tissue tumor. Journal of Surgical Oncology, 2020, 122, 1791-1801.	0.8	3
39	Structural Origin and Surgical Complications of Peripheral Schwannomas. Anticancer Research, 2020, 40, 6563-6570.	0.5	1
40	Low-grade myofibroblastic sarcoma of the levator scapulae muscle: a case report and literature review. BMC Musculoskeletal Disorders, 2020, 21, 836.	0.8	10
41	A Novel Anionic-phosphate-platinum Complex Effectively Targets a Cisplatinum-resistant Osteosarcoma in a Patient-derived Orthotopic Xenograft Mouse Model. Cancer Genomics and Proteomics, 2020, 17, 217-223.	1.0	7
42	Recombinant Methioninase Combined With Tumor-targeting <i>Salmonella typhimurium</i> A1-R Induced Regression in a PDOX Mouse Model of Doxorubicin-resistant Dedifferentiated Liposarcoma. Anticancer Research, 2020, 40, 2515-2523.	0.5	4
43	Eribulin Regresses a Doxorubicin-resistant Dedifferentiated Liposarcoma in a Patient-derived Orthotopic Xenograft Mouse Model. Cancer Genomics and Proteomics, 2020, 17, 351-358.	1.0	3
44	Recent Advances and Challenges in the Treatment of Rhabdomyosarcoma. Cancers, 2020, 12, 1758.	1.7	30
45	Pedicle frozen autograft–prosthesis composite reconstructions for malignant bone tumors of the proximal femur. BMC Musculoskeletal Disorders, 2020, 21, 81.	0.8	7
46	Exquisite Tumor Targeting by Salmonella A1-R in Combination with Caffeine and Valproic Acid Regresses an Adult Pleomorphic Rhabdomyosarcoma Patient-Derived Orthotopic Xenograft Mouse Model. Translational Oncology, 2020, 13, 393-400.	1.7	7
47	The accuracy of different FRAX tools in predicting fracture risk in Japan: A comparison study Journal of Orthopaedic Surgery, 2020, 28, 230949902091727.	0.4	4
48	Glycogen synthase kinase 3β as a potential therapeutic target in synovial sarcoma and fibrosarcoma. Cancer Science, 2020, 111, 429-440.	1.7	28
49	Delayed Initiation of Treatment Is Associated With Metastasis of Soft-tissue Sarcoma. Anticancer Research, 2020, 40, 7009-7015.	0.5	7
50	Distal Tibial Tuberosity Focal Dome Osteotomy Combined With Intra-Articular Condylar Osteotomy (Focal Dome Condylar Osteotomy) for Medial Osteoarthritis of the Knee Joint. Arthroscopy Techniques, 2020, 9, e1079-e1086.	0.5	3
51	Efficacy of the combination of fluorescence-guided surgery and adjuvant therapy in orthotopic nude mouse models of cancer. , 2020, , 45-58.		0
52	Fluorescence-guided surgery for primary and metastatic bone tumors in orthotopic nude mouse models. , 2020, , 125-137.		0
53	Cystic extraskeletal osteosarcoma: Three case reports and review of the literature. Molecular and Clinical Oncology, 2020, 12, 468-474.	0.4	4
54	Sorafenib and Palbociclib Combination Regresses a Cisplatinum-resistant Osteosarcoma in a PDOX Mouse Model. Anticancer Research, 2019, 39, 4079-4084.	0.5	24

#	Article	IF	CITATIONS
55	The Combination of Olaratumab with Doxorubicin and Cisplatinum Regresses a Chemotherapy-Resistant Osteosarcoma in a Patient-Derived Orthotopic Xenograft Mouse Model. Translational Oncology, 2019, 12, 1257-1263.	1.7	18
56	Distribution of Solitary and Multiple Enchondromas of the Hand. In Vivo, 2019, 33, 2235-2240.	0.6	9
57	Risk factors for surgical site infection after malignant bone tumor resection and reconstruction. BMC Cancer, 2019, 19, 33.	1.1	28
58	Local dissemination of osteosarcoma observed after massage therapy: a case report. BMC Cancer, 2019, 19, 993.	1.1	5
59	Pioglitazone, an agonist of PPAR ^ĵ 3, reverses doxorubicin-resistance in an osteosarcoma patient-derived orthotopic xenograft model by downregulating P-glycoprotein expression. Biomedicine and Pharmacotherapy, 2019, 118, 109356.	2.5	28
60	Combination Treatment With Sorafenib and Everolimus Regresses a Doxorubicin-resistant Osteosarcoma in a PDOX Mouse Model. Anticancer Research, 2019, 39, 4781-4786.	0.5	22
61	Treatment of a Malignant Soft Tissue Tumor Arising in the Vicinity of the Sciatic Nerve with an In-Situ Preparation Technique and Intensive Multidisciplinary Therapy. Cancers, 2019, 11, 506.	1.7	4
62	Pazopanib regresses a doxorubicin-resistant synovial sarcoma in a patient-derived orthotopic xenograft mouse model. Tissue and Cell, 2019, 58, 107-111.	1.0	3
63	Determining Patient Satisfaction and Treatment Desires in Patients With Musculoskeletal Sarcoma of the Knee After Joint-preservation Surgery Using a Questionnaire Survey. Anticancer Research, 2019, 39, 1965-1969.	0.5	4
64	Olaratumab combined with doxorubicin and ifosfamide overcomes individual doxorubicin and olaratumab resistance of an undifferentiated soft-tissue sarcoma in a PDOX mouse model. Cancer Letters, 2019, 451, 122-127.	3.2	11
65	Successful treatment of pathologic femoral shaft fracture associated with large arteriovenous malformations using a 3-dimensional external fixator and teriparatide: a case report. BMC Surgery, 2019, 19, 35.	0.6	10
66	Satisfaction After Joint-preservation Surgery in Patients With Musculoskeletal Knee Sarcoma Based on Various Scores. Anticancer Research, 2019, 39, 1959-1964.	0.5	3
67	Trabectedin and irinotecan combination regresses a cisplatinum-resistant osteosarcoma in a patient-derived orthotopic xenograft nude-mouse model. Biochemical and Biophysical Research Communications, 2019, 513, 326-331.	1.0	34
68	The combination of olaratumab with gemcitabine and docetaxel arrests a chemotherapy-resistant undifferentiated soft-tissue sarcoma in a patient-derived orthotopic xenograft mouse model. Cancer Chemotherapy and Pharmacology, 2019, 83, 1075-1082.	1.1	7
69	Osimertinib Regresses an EGFR-Mutant Cisplatinum- Resistant Lung Adenocarcinoma Growing in the Brain in Nude Mice. Translational Oncology, 2019, 12, 640-645.	1.7	10
70	Randomized placebo-controlled double-blind phase II study of zaltoprofen for patients with diffuse-type and unresectable localized tenosynovial giant cell tumors: a study protocol. BMC Musculoskeletal Disorders, 2019, 20, 68.	0.8	7
71	Oral Recombinant Methioninase, Combined With Oral Caffeine and Injected Cisplatinum, Overcome Cisplatinum-Resistance and Regresses Patient-derived Orthotopic Xenograft Model of Osteosarcoma. Anticancer Research, 2019, 39, 4653-4657.	0.5	30
72	Joint-preservation surgery for pediatric osteosarcoma of the knee joint. Cancer and Metastasis Reviews, 2019, 38, 709-722.	2.7	49

#	Article	IF	CITATIONS
73	Asymptomatic Bone Marrow Edema Detected by 67Ga Scintigraphy. Clinical Nuclear Medicine, 2019, 44, 680-682.	0.7	0
74	Current and Emerging Targets in Immunotherapy for Osteosarcoma. Journal of Oncology, 2019, 2019, 1-8.	0.6	79
75	The combination of gemcitabine and nab-paclitaxel as a novel effective treatment strategy for undifferentiated soft-tissue sarcoma in a patient-derived orthotopic xenograft (PDOX) nude-mouse model. Biomedicine and Pharmacotherapy, 2019, 111, 835-840.	2.5	10
76	Therapeutic Targets for Bone and Soft-Tissue Sarcomas. International Journal of Molecular Sciences, 2019, 20, 170.	1.8	52
77	Tumor-targeting Salmonella typhimurium A1-R is a highly effective general therapeutic for undifferentiated soft tissue sarcoma patient-derived orthotopic xenograft nude-mouse models. Biochemical and Biophysical Research Communications, 2018, 497, 1055-1061.	1.0	28
78	Clinical outcomes of radioâ€hyperthermoâ€chemotherapy for soft tissue sarcoma compared to a soft tissue sarcoma registry in Japan: a retrospective matchedâ€pair cohort study. Cancer Medicine, 2018, 7, 1560-1571.	1.3	9
79	Anti-tumor effects of a nonsteroidal anti-inflammatory drug zaltoprofen on chondrosarcoma via activating peroxisome proliferator-activated receptor gamma and suppressing matrix metalloproteinase-2 expression. Cancer Medicine, 2018, 7, 1944-1954.	1.3	21
80	Tumor-targeting Salmonella typhimurium A1-R combined with recombinant methioninase and cisplatinum eradicates an osteosarcoma cisplatinum-resistant lung metastasis in a patient-derived orthotopic xenograft (PDOX) mouse model: decoy, trap and kill chemotherapy moves toward the clinic. Cell Cycle, 2018, 17, 801-809.	1.3	57
81	Mid―to longâ€ŧerm clinical outcome of giant cell tumor of bone treated with calcium phosphate cement following thorough curettage and phenolization. Journal of Surgical Oncology, 2018, 117, 1232-1238.	0.8	16
82	Recombinant methioninase in combination with doxorubicin (DOX) overcomes first-line DOX resistance in a patient-derived orthotopic xenograft nude-mouse model of undifferentiated spindle-cell sarcoma. Cancer Letters, 2018, 417, 168-173.	3.2	56
83	Imaging DNA Repair After UV Irradiation Damage of Cancer Cells in Gelfoam® Histoculture. Methods in Molecular Biology, 2018, 1760, 199-203.	0.4	0
84	Spontaneous shrinkage of solitary osteochondromas. Skeletal Radiology, 2018, 47, 61-68.	1.2	10
85	Growth of doxorubicinâ€resistant undifferentiated spindleâ€cell sarcoma PDOX is arrested by metabolic targeting with recombinant methioninase. Journal of Cellular Biochemistry, 2018, 119, 3537-3544.	1.2	30
86	Factors Associated With Discharge Destination in Advanced Cancer Patients With Bone Metastasis in a Japanese Hospital. Annals of Rehabilitation Medicine, 2018, 42, 477-482.	0.6	2
87	Metabolic targeting with recombinant methioninase combined with palbociclib regresses a doxorubicin-resistant dedifferentiated liposarcoma. Biochemical and Biophysical Research Communications, 2018, 506, 912-917.	1.0	29
88	Growth of epiphysis after epiphyseal-preservation surgery for childhood osteosarcoma around the knee joint. BMC Musculoskeletal Disorders, 2018, 19, 185.	0.8	21
89	Oral Recombinant Methioninase Combined with Caffeine and Doxorubicin Induced Regression of a Doxorubicin-resistant Synovial Sarcoma in a PDOX Mouse Model. Anticancer Research, 2018, 38, 5639-5644.	0.5	50
90	Efficacy of radio-hyperthermo-chemotherapy as salvage therapy for recurrent or residual malignant soft tissue tumors. International Journal of Hyperthermia, 2018, 35, 658-666.	1.1	5

#	Article	IF	CITATIONS
91	The usefulness of wide excision assisted by a computer navigation system and reconstruction using a frozen bone autograft for malignant acetabular bone tumors: a report of two cases. BMC Cancer, 2018, 18, 1036.	1.1	11
92	Treatment of aneurysmal bone cysts using endoscopic curettage. BMC Musculoskeletal Disorders, 2018, 19, 268.	0.8	23
93	Treatment of simple bone cysts using endoscopic curettage: a case series analysis. Journal of Orthopaedic Surgery and Research, 2018, 13, 168.	0.9	20
94	Efficacy and Limitations of F-18-fluoro-2-deoxy-D-glucose Positron Emission Tomography to Differentiate Between Malignant and Benign Bone and Soft Tissue Tumors. Anticancer Research, 2018, 38, 4065-4072.	0.5	2
95	Preoperative evaluation of the efficacy of radio-hyperthermo-chemotherapy for soft tissue sarcoma in a case series. PLoS ONE, 2018, 13, e0195289.	1.1	5
96	Treatment outcomes of the simple bone cyst. Medicine (United States), 2018, 97, e0572.	0.4	10
97	Temozolomide regresses a doxorubicinâ€resistant undifferentiated spindleâ€cell sarcoma patientâ€derived orthotopic xenograft (PDOX): precisionâ€oncology nudeâ€mouse model matching the patient with effective therapy. Journal of Cellular Biochemistry, 2018, 119, 6598-6603.	1.2	14
98	Temozolomide combined with irinotecan regresses a cisplatinum-resistant relapsed osteosarcoma in a patient-derived orthotopic xenograft (PDOX) precision-oncology mouse model. Oncotarget, 2018, 9, 7774-7781.	0.8	22
99	Recombinant methioninase combined with doxorubicin (DOX) regresses a DOX-resistant synovial sarcoma in a patient-derived orthotopic xenograft (PDOX) mouse model. Oncotarget, 2018, 9, 19263-19272.	0.8	22
100	The Efficacy of Wide Resection for Musculoskeletal Metastatic Lesions of Renal Cell Carcinoma. Anticancer Research, 2018, 38, 577-582.	0.5	6
101	Calcium Phosphate Cement in the Surgical Management of Benign Bone Tumors. Anticancer Research, 2018, 38, 3031-3035.	0.5	6
102	Practical use of imaging technique for management of bone and soft tissue tumors. Journal of Orthopaedic Science, 2017, 22, 391-400.	0.5	32
103	GFP labeling kinetics of triple-negative human breast cancer by a killer-reporter adenovirus in 3D Gelfoam® histoculture. In Vitro Cellular and Developmental Biology - Animal, 2017, 53, 479-482.	0.7	3
104	Phase 1/2 study of immunotherapy with dendritic cells pulsed with autologous tumor lysate in patients with refractory bone and soft tissue sarcoma. Cancer, 2017, 123, 1576-1584.	2.0	65
105	Do Mesenchymal Stem Cells Derived From Atypical Lipomatous Tumors Have Greater Differentiation Potency Than Cells From Normal Adipose Tissues?. Clinical Orthopaedics and Related Research, 2017, 475, 1693-1701.	0.7	9
106	High Efficacy of Pazopanib on an Undifferentiated Spindle-Cell Sarcoma Resistant to First-Line Therapy Is Identified With a Patient-Derived Orthotopic Xenograft (PDOX) Nude Mouse Model. Journal of Cellular Biochemistry, 2017, 118, 2739-2743.	1.2	34
107	Intra-arterial administration of tumor-targeting <i>Salmonella typhimurium</i> A1-R regresses a cisplatin-resistant relapsed osteosarcoma in a patient-derived orthotopic xenograft (PDOX) mouse model. Cell Cycle, 2017, 16, 1164-1170.	1.3	49
108	Knee joint preservation surgery in osteosarcoma using tumour-bearing bone treated with liquid nitrogen. International Orthopaedics, 2017, 41, 2189-2197.	0.9	18

#	Article	IF	CITATIONS
109	Sequential histological findings and clinical response after carbon ion radiotherapy for unresectable sarcoma. Clinical and Translational Radiation Oncology, 2017, 2, 41-45.	0.9	4
110	Experience of total scapular excision for musculoskeletal tumor and reconstruction in eastern Asian countries. Journal of Bone Oncology, 2017, 9, 55-58.	1.0	6
111	An unusual case of proximal humeral simple bone cyst in an adult from secondary cystic change. World Journal of Surgical Oncology, 2017, 15, 102.	0.8	5
112	Patient-derived orthotopic xenograft (PDOX) mouse model of adult rhabdomyosarcoma invades and recurs after resection in contrast to the subcutaneous ectopic model. Cell Cycle, 2017, 16, 91-94.	1.3	41
113	Current status of immunotherapy for sarcomas. Immunotherapy, 2017, 9, 1331-1338.	1.0	14
114	Functional and radiological outcomes of a minimally invasive surgical approach to monostotic fibrous dysplasia. World Journal of Surgical Oncology, 2017, 15, 1.	0.8	41
115	Risk factors for postoperative deep infection in bone tumors. PLoS ONE, 2017, 12, e0187438.	1.1	8
116	Temozolomide combined with irinotecan caused regression in an adult pleomorphic rhabdomyosarcoma patient-derived orthotopic xenograft (PDOX) nude-mouse model. Oncotarget, 2017, 8, 75874-75880.	0.8	33
117	A novel anionic-phosphate-platinum complex effectively targets an undifferentiated pleomorphic sarcoma better than cisplatinum and doxorubicin in a patient-derived orthotopic xenograft (PDOX). Oncotarget, 2017, 8, 63353-63359.	0.8	24
118	Pathogenesis of Osteosclerotic Change Following Treatment with an Antibody Against RANKL for Giant Cell Tumour of the Bone. Anticancer Research, 2017, 37, 748-754.	0.5	10
119	Antimetastatic Efficacy of the Combination of Caffeine and Valproic Acid on an Orthotopic Human Osteosarcoma Cell Line Model in Nude Mice. Anticancer Research, 2017, 37, 1005-1012.	0.5	10
120	Efficacy In Vitro of Caffeine and Valproic Acid on Patient-Derived Undifferentiated Pleomorphic Sarcoma and Rhabdomyosarcoma Cell Lines. Anticancer Research, 2017, 37, 4081-4084.	0.5	5
121	Effective Metabolic Targeting of Human Osteosarcoma Cells In Vitro and in Orthotopic Nude-mouse Models with Recombinant Methioninase. Anticancer Research, 2017, 37, 4807-4812.	0.5	16
122	Fluorescenceâ€guided surgery of human prostate cancer experimental bone metastasis in nude mice using anti EA DyLight 650 for tumor illumination. Journal of Orthopaedic Research, 2016, 34, 559-565.	1.2	7
123	Eradication of osteosarcoma by fluorescence-guided surgery with tumor labeling by a killer-reporter adenovirus. Journal of Orthopaedic Research, 2016, 34, 836-844.	1.2	18
124	The outcomes of reconstruction using frozen autograft combined with iodine-coated implants for malignant bone tumors: compared with non-coated implants. Japanese Journal of Clinical Oncology, 2016, 46, 735-740.	0.6	12
125	Surgical management of proximal fibular tumors: A report of 12 cases. Journal of Bone Oncology, 2016, 5, 163-166.	1.0	14
126	Clinical relevance of peroxisome proliferator-activated receptor-gamma expression in myxoid liposarcoma. BMC Cancer, 2016, 16, 442.	1.1	6

#	Article	IF	CITATIONS
127	A case of infected schwannoma mimicking malignant tumor. World Journal of Surgical Oncology, 2016, 14, 302.	0.8	4
128	Radiological assessment of the femoral bowing in Japanese population. Sicot-j, 2016, 2, 2.	0.8	39
129	Realâ€Time In Vivo Confocal Fluorescence Imaging of Prostate Cancer Boneâ€Marrow Micrometastasis Development at the Cellular Level in Nude Mice. Journal of Cellular Biochemistry, 2016, 117, 2533-2537.	1.2	4
130	The linea aspera as a guide for femoral rotation after tumor resection: is it directly posterior? A technical note. Journal of Orthopaedics and Traumatology, 2016, 17, 255-259.	1.0	7
131	Tenosynovial giant cell tumors in unusual locations detected by positron emission tomography imaging confused with malignant tumors: report of two cases. BMC Musculoskeletal Disorders, 2016, 17, 180.	0.8	18
132	Improved Resection and Outcome of Colon-Cancer Liver Metastasis with Fluorescence-Guided Surgery Using In Situ GFP Labeling with a Telomerase-Dependent Adenovirus in an Orthotopic Mouse Model. PLoS ONE, 2016, 11, e0148760.	1.1	35
133	Fluorescence-guided surgery of a highly-metastatic variant of human triple-negative breast cancer targeted with a cancer-specific GFP adenovirus prevents recurrence. Oncotarget, 2016, 7, 75635-75647.	0.8	16
134	Efficacy of glycogen synthase kinase-3β targeting against osteosarcoma via activation of β-catenin. Oncotarget, 2016, 7, 77038-77051.	0.8	23
135	Non-toxic Efficacy of the Combination of Caffeine and Valproic Acid on Human Osteosarcoma Cells In Vitro and in Orthotopic Nude-mouse Models. Anticancer Research, 2016, 36, 4477-4482.	0.5	7
136	Clinical Outcome of Reconstruction Using Frozen Autograft for a Humeral Bone Tumor. Anticancer Research, 2016, 36, 6631-6636.	0.5	16
137	Protein kinase A and Epac activation by cAMP regulates the expression of glial fibrillary acidic protein in glial cells. Archives of Biological Sciences, 2016, 68, 795-801.	0.2	7
138	Balancing Prolonged Survival with QoL Using Low-dose Pazopanib Maintenance: A Comparison with the PALETTE Study. Anticancer Research, 2016, 36, 2893-7.	0.5	10
139	Use of αv Integrin Linked to Green Fluorescent Protein in Osteosarcoma Cells and Confocal Microscopy to Image Molecular Dynamics During Lung Metastasis in Nude Mice. Anticancer Research, 2016, 36, 3811-6.	0.5	2
140	In Vivo Isolation of a Highly-aggressive Variant of Triple-negative Human Breast Cancer MDA-MB-231 Using Serial Orthotopic Transplantation. Anticancer Research, 2016, 36, 3817-20.	0.5	7
141	Efficacy of the Combination of a PARP Inhibitor and UVC on Cancer Cells as Imaged by Focus Formation by the DNA Repair-related Protein 53BP1 Linked to Green Fluorescent Protein. Anticancer Research, 2016, 36, 3821-6.	0.5	2
142	Frozen Autograft-Prosthesis Composite Reconstruction in Malignant Bone Tumors. Orthopedics, 2015, 38, e911-8.	0.5	22
143	Precise navigation surgery of tumours in the lung in mouse models enabled by in situ fluorescence labelling with a killer-reporter adenovirus. BMJ Open Respiratory Research, 2015, 2, e000096.	1.2	29
144	Realâ€Time Fluorescence Imaging of the DNA Damage Repair Response During Mitosis. Journal of Cellular Biochemistry, 2015, 116, 661-666.	1.2	1

#	Article	IF	CITATIONS
145	Successful correction of tibial bone deformity through multiple surgical procedures, liquid nitrogen-pretreated bone tumor autograft, three-dimensional external fixation, and internal fixation in a patient with primary osteosarcoma: a case report. BMC Surgery, 2015, 15, 124.	0.6	3
146	Symptomatic small schwannoma is a risk factor for surgical complications and correlates with difficulty of enucleation. SpringerPlus, 2015, 4, 751.	1.2	11
147	Risk Factors of Recurrent Lumbar Disk Herniation. Journal of Spinal Disorders and Techniques, 2015, 28, E265-E269.	1.8	70
148	Epiphyseal Sparing and Reconstruction by Frozen Bone Autograft after Malignant Bone Tumor Resection in Children. Sarcoma, 2015, 2015, 1-8.	0.7	20
149	Tumor-targeting <i>Salmonella typhimurium</i> A1-R inhibits human prostate cancer experimental bone metastasis in mouse models. Oncotarget, 2015, 6, 31335-31343.	0.8	12
150	Establishment of a Patient-Derived Orthotopic Xenograft (PDOX) Model of HER-2-Positive Cervical Cancer Expressing the Clinical Metastatic Pattern. PLoS ONE, 2015, 10, e0117417.	1.1	105
151	Tumor-Targeting Salmonella typhimurium A1-R in Combination with Trastuzumab Eradicates HER-2-Positive Cervical Cancer Cells in Patient-Derived Mouse Models. PLoS ONE, 2015, 10, e0120358.	1.1	49
152	Ten-Year Follow-Up of Desarthrodesis of the Knee Joint 41 Years after Original Arthrodesis for a Bone Tumor. Case Reports in Orthopedics, 2015, 2015, 1-6.	0.1	1
153	Treatment of a Simple Bone Cyst Using a Cannulated Hydroxyapatite Pin. Medicine (United States), 2015, 94, e1027.	0.4	19
154	Cell-cycle fate-monitoring distinguishes individual chemosensitive and chemoresistant cancer cells in drug-treated heterogeneous populations demonstrated by real-time FUCCI imaging. Cell Cycle, 2015, 14, 621-629.	1.3	23
155	Color-coding cancer and stromal cells with genetic reporters in a patient-derived orthotopic xenograft (PDOX) model of pancreatic cancer enhances fluorescence-guided surgery. Cancer Gene Therapy, 2015, 22, 344-350.	2.2	50
156	Cancer cells mimic <i>in vivo</i> spatial-temporal cell-cycle phase distribution and chemosensitivity in 3-dimensional Gelfoam® histoculture but not 2-dimensional culture as visualized with real-time FUCCI imaging. Cell Cycle, 2015, 14, 808-819.	1.3	33
157	Heterogeneous cell-cycle behavior in response to UVB irradiation by a population of single cancer cells visualized by time-lapse FUCCI imaging. Cell Cycle, 2015, 14, 1932-1937.	1.3	6
158	Experimental Curative Fluorescence-guided Surgery of Highly Invasive Glioblastoma Multiforme Selectively Labeled With a Killer-reporter Adenovirus. Molecular Therapy, 2015, 23, 1182-1188.	3.7	37
159	Fluorescence-Guided Surgery of Retroperitoneal-Implanted Human Fibrosarcoma in Nude Mice Delays or Eliminates Tumor Recurrence and Increases Survival Compared to Bright-Light Surgery. PLoS ONE, 2015, 10, e0116865.	1.1	10
160	Tumor-Targeting Salmonella typhimurium A1-R Arrests a Chemo-Resistant Patient Soft-Tissue Sarcoma in Nude Mice. PLoS ONE, 2015, 10, e0134324.	1.1	78
161	Tumor-targetingSalmonella typhimuriumA1-R arrests growth of breast-cancer brain metastasis. Oncotarget, 2015, 6, 2615-2622.	0.8	59
162	Intraperitoneal administration of tumor-targeting <i>Salmonella typhimurium</i> A1-R inhibits disseminated human ovarian cancer and extends survival in nude mice. Oncotarget, 2015, 6, 11369-11377.	0.8	55

#	Article	IF	CITATIONS
163	Targeting tumors with a killer-reporter adenovirus for curative fluorescence-guided surgery of soft-tissue sarcoma. Oncotarget, 2015, 6, 13133-13148.	0.8	45
164	Effectiveness of Two Novel Anionic and Cationic Platinum Complexes in the Treatment of Osteosarcoma. Anti-Cancer Agents in Medicinal Chemistry, 2015, 15, 390-399.	0.9	11
165	Cell-cycle fate-monitoring to identify individual chemosensitive and chemoresistant cancer cells in heterogeneous cancer populations Journal of Clinical Oncology, 2015, 33, e13514-e13514.	0.8	0
166	Prevention of experimental human breast cancer bone metastasis in nude mice by tumor-targeting <i>Salmonella typhimurium </i> A1-R Journal of Clinical Oncology, 2015, 33, e13513-e13513.	0.8	0
167	Inhibition of soft-tissue sarcoma lung metastasis by tumor-targeting Salmonella typhimurium A1-R Journal of Clinical Oncology, 2015, 33, e13515-e13515.	0.8	0
168	Abstract 3241: Tumor-targeting Salmonella typhimurium A1-R inhibits peritoneal dissemination of ovarian cancer and prolongs survival of the tumor-bearing nude mice. , 2015, , .		0
169	Abstract 5117: Fluorescence-guided surgery of liver metastasis in orthotopic nude-mouse models. , 2015, , .		0
170	Abstract 5123: Curative fluorescence-guided surgery of pancreatic cancer in combination with UVC irradiation in orthotopic mouse models. , 2015, , .		0
171	Patient-derived orthotopic xenograft (PDOX) nude mouse model of soft-tissue sarcoma more closely mimics the patient behavior in contrast to the subcutaneous ectopic model. Anticancer Research, 2015, 35, 697-701.	0.5	63
172	Fluorescence-Guided Surgery in Combination with UVC Irradiation Cures Metastatic Human Pancreatic Cancer in Orthotopic Mouse Models. PLoS ONE, 2014, 9, e99977.	1.1	26
173	The Tumor-Educated-Macrophage Increase of Malignancy of Human Pancreatic Cancer Is Prevented by Zoledronic Acid. PLoS ONE, 2014, 9, e103382.	1.1	15
174	Efficacy of tumor-targeting Salmonella typhimurium A1-R in combination with anti-angiogenesis therapy on a pancreatic cancer patient-derived orthotopic xenograft (PDOX) and cell line mouse models. Oncotarget, 2014, 5, 12346-12357.	0.8	128
175	Real Time Color Coded Imaging of Cell Cycle Phase Demonstrates Why Invasive Metastatic Cancer Cells are Drug Resistant. Annals of Oncology, 2014, 25, v50.	0.6	0
176	Pancreatic Cancer Patient-Derived Orthotopic Xenograft (Pdox) Cured by Fluorescence-Guided Surgery Followed by Uvc. Annals of Oncology, 2014, 25, v62.	0.6	0
177	Fluorescence-Guided Surgery of Pancreatic Patient-Derived Orthotopic Xenograft(Pdox) with a Portable Imaging System. Annals of Oncology, 2014, 25, v93.	0.6	0
178	Efficacy of Tumor-Targeting Salmonella Typhimurium A1-R on Highly Metastatic Human Pancreatic Cancer in Nude Mice. Annals of Oncology, 2014, 25, v94.	0.6	0
179	Theobromine, the Primary Methylxanthine Found in <i>Theobroma cacao</i> , Prevents Malignant Glioblastoma Proliferation by Negatively Regulating Phosphodiesterase-4, Extracellular Signal-regulated Kinase, Akt/mammalian Target of Rapamycin Kinase, and Nuclear Factor-Kappa B. Nutrition and Cancer. 2014. 66. 419-423.	0.9	57
180	Tumor-targeting <i>Salmonella typhimurium</i> A1-R decoys quiescent cancer cells to cycle as visualized by FUCCI imaging and become sensitive to chemotherapy. Cell Cycle, 2014, 13, 3958-3963.	1.3	96

#	Article	IF	CITATIONS
181	Spatial–temporal FUCCI imaging of each cell in a tumor demonstrates locational dependence of cell cycle dynamics and chemoresponsiveness. Cell Cycle, 2014, 13, 2110-2119.	1.3	69
182	Osteosarcoma Cells Enhance Angiogenesis Visualized by Colorâ€Coded Imaging in the In Vivo Gelfoam® Assay. Journal of Cellular Biochemistry, 2014, 115, 1490-1494.	1.2	11
183	Efficacy of tumor-targetingSalmonella typhimuriumA1-R on nude mouse models of metastatic and disseminated human ovarian cancer. Journal of Cellular Biochemistry, 2014, 115, n/a-n/a.	1.2	47
184	Comparison of UVB and UVC Effects on the DNA Damageâ€Response Protein 53BP1 in Human Pancreatic Cancer. Journal of Cellular Biochemistry, 2014, 115, 1724-1728.	1.2	19
185	Efficacy of <i>Salmonella typhimurium</i> A1â€R Versus Chemotherapy on a Pancreatic Cancer Patientâ€Derived Orthotopic Xenograft (PDOX). Journal of Cellular Biochemistry, 2014, 115, 1254-1261.	1.2	93
186	Fluorescence-guided surgery improves outcome in an orthotopic osteosarcoma nude-mouse model. Journal of Orthopaedic Research, 2014, 32, 1596-1601.	1.2	26
187	Successful Fluorescence-Guided Surgery on Human Colon Cancer Patient-Derived Orthotopic Xenograft Mouse Models Using a Fluorophore-Conjugated Anti-CEA Antibody and a Portable Imaging System. Journal of Laparoendoscopic and Advanced Surgical Techniques - Part A, 2014, 24, 241-247.	0.5	117
188	Hand-held high-resolution fluorescence imaging system for fluorescence-guided surgery of patient and cell-line pancreatic tumors growing orthotopically in nude mice. Journal of Surgical Research, 2014, 187, 510-517.	0.8	71
189	Diagnosis and treatment of low-grade osteosarcoma: experience with nine cases. International Journal of Clinical Oncology, 2014, 19, 731-738.	1.0	18
190	Invading cancer cells are predominantly in G ₀ /G ₁ resulting in chemoresistance demonstrated by real-time FUCCI imaging. Cell Cycle, 2014, 13, 953-960.	1.3	67
191	Fluorescence-guided surgery of prostate cancer bone metastasis. Journal of Surgical Research, 2014, 192, 124-133.	0.8	13
192	Late Recurrence of Osteosarcoma: A Report of Two Cases. Journal of Orthopaedic Surgery, 2014, 22, 415-419.	0.4	3
193	Abstract 1218: Telomerase-specific GFP-expressing adenovirus enables fluorescence-guided surgery (FGS) for patient-derived orthotopic xenograft (PDOX) in nude mice. Cancer Research, 2014, 74, 1218-1218.	0.4	1
194	Tumor-targeting <i>Salmonella typhimurium</i> A1-R prevents experimental human breast cancer bone metastasis in nude mice. Oncotarget, 2014, 5, 7119-7125.	0.8	34
195	Inhibition of spontaneous and experimental lung metastasis of soft-tissue sarcoma by tumor-targeting Salmonella typhimurium A1-R. Oncotarget, 2014, 5, 12849-12861.	0.8	39
196	Theobromine, the primary methylxanthine found in Theobroma cacao, inhibits malignant glioblastoma cell growth by negatively regulating Akt/mammalian target of rapamycin kinase (LB836). FASEB Journal, 2014, 28, LB836.	0.2	1
197	Prognostic value of novel combined scoring system in patients with high-grade soft tissue sarcoma Journal of Clinical Oncology, 2014, 32, e21523-e21523.	0.8	0
198	Impact of excision repair cross-complementation group 1 (ERCC1) protein on survival of patients with osteosarcoma treated with cisplatin-based chemotherapy Journal of Clinical Oncology, 2014, 32, 10535-10535.	0.8	0

#	Article	IF	CITATIONS
199	Prognostic value of peroxisome proliferator-activated receptor gamma expression on clinical outcome of myxoid liposarcoma Journal of Clinical Oncology, 2014, 32, 10574-10574.	0.8	0
200	A hand-held portable imaging system for effective fluorescence-guided surgery of a pancreatic patient-derived orthotopic xenograft (PDOX) in nude mice Journal of Clinical Oncology, 2014, 32, e15219-e15219.	0.8	0
201	Effect of fluorescence-guided surgery followed by UVC on a pancreatic cancer patient-derived orthotopic xenograft (PDOX) in nude mice Journal of Clinical Oncology, 2014, 32, e15220-e15220.	0.8	0
202	Effect of Salmonella typhimurium A1-R on a pancreatic cancer patient-derived orthotopic xenograft (PDOX) in nude mice Journal of Clinical Oncology, 2014, 32, e15218-e15218.	0.8	0
203	Efficacy of novel proteasome inhibitory platinum complex against osteosarcoma Journal of Clinical Oncology, 2014, 32, 10534-10534.	0.8	0
204	Abstract 3486: Efficacy of neoadjuvant chemotherapy in combination with fluorescence-guided surgery on a pancreatic cancer patient-derived orthotopic xenograft (PDOX). , 2014, , .		0
205	Abstract 1982: Invading cancer cells are mostly in GO/G1 and resist chemotherapy demonstrated by real-time FUCCI imaging of cell-cycle kinetics in Gelfoam® histoculture. , 2014, , .		0
206	Abstract 1204: Establishment of a patient-derived orthotopic xenograft (PDOX) model of patient cervical cancer. , 2014, , .		0
207	Abstract 3130: Zoledronic acid inhibits proliferation and metastasis of human pancreatic cancer in the patient-derived orthotopic xenograft (PDOX) model by targeting tumor-educated macrophages. , 2014, , . •		0
208	Abstract 1230: Efficacy of Salmonella typhimurium A1-R and anti-VEGF therapy on a patient-derived orthotopic xenograft (PDOX) pancreatic cancer model. , 2014, , .		0
209	Abstract 1229: The advantages of patient-derived orthotopic xenograft (PDOX) of metastatic cervical cancer for individualized therapy compared to the PDX model. , 2014, , .		0
210	Abstract 5: Real-timein vivoimaging of osteosarcoma angiogenesis. , 2014, , .		0
211	Abstract 4313: Efficacy of fluorescence-guided surgery on primary human osteosarcoma. , 2014, , .		0
212	Abstract 4375: UVC irradiation in combination with fluorescence-guided surgery cures metastatic human pancreatic cancer in orthotopic mouse models. , 2014, , .		0
213	Abstract 5095: Real-time FUCCI imaging of cell cycle phase in tumors demonstrates why cancer chemotherapy is not effective in solid cancers. , 2014, , .		0
214	Abstract 2384: Time-lapse imaging of response to DNA damage occuring during mitosis. , 2014, , .		0
215	Abstract 13: Color-coded imaging of vessel anastomosisin vivousing RFP and CFP transgenic mice. , 2014, , .		0
216	Abstract 1979: Three-dimensional Gelfoam® histoculture enables cancer cells to mimicin vivocancer cell cycling as visualized with FUCCI imaging. , 2014, , .		0

#	Article	IF	CITATIONS
217	Abstract 711: Salmonella typhimurium A1-R induces quiescent FUCCI-expressing cancer cells to cycle and become chemosensitive. , 2014, , .		0
218	Abstract 1983: Real-time imaging of exosomes dynamic of cross-talking and cell trafficking in 3D Gelfoam® histoculture. , 2014, , .		0
219	Abstract A40: Pancreatic cancer patient-derived orthotopic xenograft (PDOXâ"¢) is effectively targeted bySalmonella typhimuriumA1-R. , 2014, , .		0
220	Abstract B01: A portable imaging system for fluorescence-guided surgery on a human colon cancer patient-derived orthotopic xenograft (PDOXâ,,¢) nude mouse model. , 2014, , .		0
221	Outcomes and complications of reconstruction using tumor-bearing frozen autografts in patients with metastatic bone tumors. Anticancer Research, 2014, 34, 5569-77.	0.5	7
222	Dynamic color-coded fluorescence imaging of the cell-cycle phase, mitosis, and apoptosis demonstrates how caffeine modulates cisplatinum efficacy. Journal of Cellular Biochemistry, 2013, 114, 2454-2460.	1.2	21
223	Imaging UVC-induced DNA damage response in models of minimal cancer. Journal of Cellular Biochemistry, 2013, 114, 2493-2499.	1.2	20
224	Comparison of efficacy ofSalmonella typhimuriumA1-R and chemotherapy on stem-like and non-stem human pancreatic cancer cells. Cell Cycle, 2013, 12, 2774-2780.	1.3	78
225	Targeted activation of PKA and Epac promotes glioblastoma regression in vitro. Molecular and Clinical Oncology, 2013, 1, 281-285.	0.4	15
226	Huge and deeply situated glomus tumor. Current Orthopaedic Practice, 2013, 24, 670-673.	0.1	0
227	Nestin-Expressing Stem Cells Promote Nerve Growth in Long-Term 3-Dimensional Gelfoam®-Supported Histoculture. PLoS ONE, 2013, 8, e67153.	1.1	38
228	Prognostic Value of Radiological Response to Chemotherapy in Patients with Osteosarcoma. PLoS ONE, 2013, 8, e70015.	1.1	15
229	Prognostic Value of Histological Response to Chemotherapy in Osteosarcoma Patients Receiving Tumor-Bearing Frozen Autograft. PLoS ONE, 2013, 8, e71362.	1.1	27
230	Abstract A92: Killing quiescent cancer cells in vitro and in vivo with tumor targetingSalmonella typhimuriumA1-R. , 2013, , .		0
231	Abstract A41: Cancer cells invade or divide, not both. , 2013, , .		1
232	Abstract A40: Cancer cells form in vivo-like tumors in Gelfoam histoculture. , 2013, , .		0
233	Effect of dormant cancer cells on angiogenesis after resisting chemotherapy Journal of Clinical Oncology, 2013, 31, e13577-e13577.	0.8	0
234	Abstract B13: Salmonella typhimurium A1-R targets human pancreatic cancer patient-derived orthotopic xenograft (PDOX) in nude mice , 2013, , .		0

#	Article	IF	CITATIONS
235	Abstract B60: FUCCI cell cycle imaging identifies drug-resistant quiescent cancer cells within tumors , 2013, , .		0
236	A color-coded imaging model of the interaction of αv integrin-GFP expressed in osteosarcoma cells and RFP expressing blood vessels in Gelfoam® vascularized in vivo. Anticancer Research, 2013, 33, 1361-6.	0.5	8
237	Single cell time-lapse imaging of focus formation by the DNA damage-response protein 53BP1 after UVC irradiation of human pancreatic cancer cells. Anticancer Research, 2013, 33, 1373-7.	0.5	14
238	Color-coded imaging of spontaneous vessel anastomosis in vivo. Anticancer Research, 2013, 33, 3041-5.	0.5	6
239	A novel combined radiological method for evaluation of the response to chemotherapy for primary bone sarcoma. Journal of Surgical Oncology, 2012, 106, 273-279.	0.8	13
240	TNF-α and Tumor Lysate Promote the Maturation of Dendritic Cells for Immunotherapy for Advanced Malignant Bone and Soft Tissue Tumors. PLoS ONE, 2012, 7, e52926.	1.1	16
241	Efficacy of newly developed platinum complexes against osteosarcoma, bone-targeting platinum, and proteasome inhibitory platinum Journal of Clinical Oncology, 2012, 30, 10075-10075.	0.8	0
242	Caffeine induces apoptosis of osteosarcoma cells by inhibiting AKT/mTOR/S6K, NF-κB and MAPK pathways. Anticancer Research, 2012, 32, 3643-9.	0.5	40
243	Activity of bone morphogenetic protein-7 after treatment at various temperatures: Freezing vs. pasteurization vs. allograft. Cryobiology, 2011, 63, 235-239.	0.3	67
244	Activation of tumor suppressor protein PTEN and induction of apoptosis are involved in cAMP-mediated inhibition of cell number in B92 glial cells. Neuroscience Letters, 2011, 497, 55-59.	1.0	18
245	Caffeine activates tumor suppressor PTEN in sarcoma cells. International Journal of Oncology, 2011, 39, 465-72.	1.4	24
246	Use of 99mTc-MIBI scintigraphy in the evaluation of the response to chemotherapy for osteosarcoma: comparison with 201Tl scintigraphy and angiography. International Journal of Clinical Oncology, 2011, 16, 373-378.	1.0	14
247	Functional outcomes after total scapulectomy for malignant bone or soft tissue tumors in the shoulder girdle. International Journal of Clinical Oncology, 2011, 16, 568-573.	1.0	22
248	Desmoplastic small round cell tumour successfully treated with caffeine-assisted chemotherapy: a case report and review of the literature. Anticancer Research, 2010, 30, 3769-74.	0.5	11
249	Lowâ€grade malignant softâ€tissue perineurioma: Interphase fluorescence <i>in situ</i> hybridization. Pathology International, 2008, 58, 718-722.	0.6	14
250	Studies on bile secretion (III) the uptake, conjugation and excretion of bile pigments by the liver under the obstructive jaundice. Gastroenterologia Japonica, 1968, 3, 298-298.	0.4	0
251	Hepatic fibrosis: Histologic and histochemical studies about chronic alcoholic and viral liver injuries and mast cell in connective tissue. Gastroenterologia Japonica, 1966, 1, 58-58.	0.4	0
252	Studies on leucine aminopeptidase. Gastroenterologia Japonica, 1966, 1, 50-51.	0.4	0